CHARACTERISTICS AND RADIATION TOLERANCE OF A DOUBLE-SIDED MICROSTRIP DETECTOR WITH POLYSILICON BIASING RESISTORS

A.P. de Haas, P. Kuijer
Utrecht University, The Netherlands

V.I. Kulibaba, N.I. Maslov, V.L. Perevertailo, V.D. Ovchinnik, S.M. Potin, A.F. Starodubtsev
National Science Center "Kharkov Institute of Physics and Technology", Kharkov, Ukraine

The characteristics and radiation tolerance of a double-sided microstrip detector (DSMD) were studied, and the suitability of the detector to the ALICE experiment requirements was analyzed. The sensitive area of the silicon microstrip detector measures 40×75 mm. The DSMD consists of 750 registering strips on each side. The strip pitch is 100 μm and the strip length is 40 mm. Strips of the p^+-side were oriented parallel to the side edge, the n^+-strips were placed at 30 mrad stereo angle with respect to p^+-strips and were separated by a common p^+-stop structure. Both p^+- and n^+-strips are biased by integrated polysilicon resistors with a resistance no less than 10 MOhm. The data readout is realized with use of 120 pF coupling capacitors.

The radiation tolerance of the microstrip detector was studied using 20 MeV electrons. The leakage current increases from 2 up to 5 nA per one strip and the interstrip resistance decreases from 43 down to 30 GOhm after 10 krad irradiation dose. The other DSMD features remain unchanged under irradiation.

To evaluate the detector efficiency, the yield of good coupling capacitors and biasing resistors, as well as strip leakage currents, interstrip resistance and interstrip capacitance were studied. Based on the data obtained, the number of defective strips is found not to exceed 3%; this provides the required detector efficiency of about 97%.

PACS: 29.40.Wk

1. INTRODUCTION

The full-scale prototype of microstrip detector for ALICE experiments has been developed and manufactured since 1996. By now, three batches of microstrip detectors have been manufactured. The single-sided detectors of the first two batches were used to investigate the influence of an additional insulating Si_3N_4 layer on leakage currents, the breakdown voltage of coupling capacitors, the interstrip resistance, etc. [1].

The single-sided microstrip detector was developed to be the p^+-side of the double-sided microstrip detector. In 1998, the full-scale prototype of a DSMD was manufactured; studies were made of the static characteristics of the detector and their behavior under a 10-year dose of the ALICE experiment. The results of the development and studies on static characteristics of the two-coordinate detector prototype are presented in this note.

2. DETECTOR DESIGN

To ensure a comprehensive study of the detector's static characteristics and to provide the control of the technological process, three groups of test structures for microstrip, diode and technological test structures on a 4" silicon wafer were designed and manufactured. The test structures surround the full-scale DSMD located at the center of the wafer (Fig. 1).

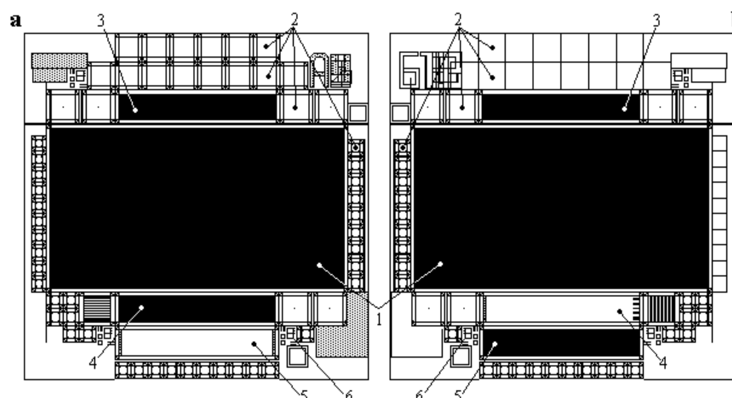

***Fig. 1**. p^+-side (**a**) and n^+-side (**b**) of 4-inch wafer with microstrip detector (1) and test structures: 2- diodes, 3-5- microstrip test structures, 6- technological test structures.*

ВОПРОСЫ АТОМНОЙ НАУКИ И ТЕХНИКИ. 2000, № 2.
Серия: Ядерно-физические исследования (36), с. 26-33.

2.1. DOUBLE-SIDED DETECTOR

The sensitive area of the double-sided (DSMD) silicon microstrip detector measures 40×75 mm^2. The DSMD consists of 750 registering strips on each side. The strip pitch is 100 μm and the strip length is 40 mm. Strips of the p^+-side were oriented parallel to the side edge, the n^+-strips were placed at a 30 mrad stereo angle with respect to p^+-strips (Fig. 2). The n^+-strips are separated with the common p^+- stop structure to exclude the connection of n^+-strips by the accumulation layer. Both p^+- and n^+-strips are biased by integrated polysilicon resistors with a resistance no less than 10 MOhm. The data readout is realized using 120 pF coupling capacitors. The insulating layer for coupling capacitors is 0.250 μm of silicon oxide. Two contact pads on each side of strips are situated in two rows to ensure the module repairability. Detector protection against mechanical and atmospheric effects is ensured by the 1 μm passivating layer of silicon oxide. One opens up areas in the passivating layer only to Al contact pads of p-strips, coupling capacitors, guard rings and biasing line of integrated resistors.

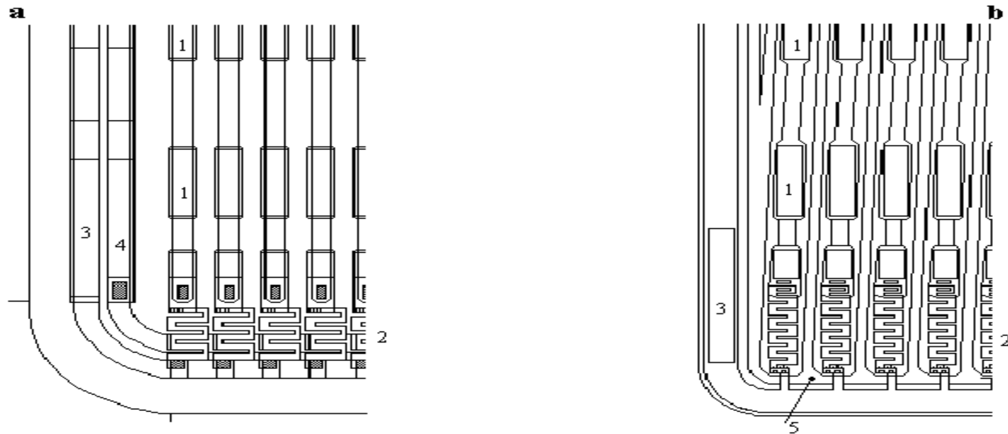

Fig. 2. *Microstrip detector corners of the double-sided detector (**a**- p^+side, **b**- n^+side):*
1- coupling capacitor pads, 2- polysilicon resistors, 3- biasing pads, 4- p^+-guard ring, 5- p^+-stop structure.

2.2. TEST MICROSTRIP STRUCTURES

Simultaneously with the main double-sided microstrip detector, three microstrip test structures located at the edges of the plate have been manufactured (Fig. 1). The first test microstrip structure is a double-sided microstrip detector with 64 registering strips on each side loaded by integrated resistors. With the exception of the decreased number of strips the test structure corresponds to a full-scale detector. The second test microstrip structure (4) is a single-sided p^+-microstrip detector with 64 strips loaded by integrated resistors. The third test structure (5) is a 64-strips single-sided n^+-detector with integrated polysilicon resistors and integrated coupling capacitors.

All these three test structures, like the main detector, are surrounded by guard rings and coated with a passivating layer.

The microstrip test structures are provided for studying signal spectrum, space resolution and their variation under irradiation.

2.3. DIODE TEST STRUCTURES

Microstrip detector and microstrip test structures are surrounded by diode test structures (Fig. 1).

The diode test structures serve for studying the quality of silicon, for measuring the depleting voltage by a capacitive technique, for preliminary studies of the microstrip detector characteristics and evaluation of their behavior under irradiation. Their application permits one to reduce the necessary number of microstrip detectors at the stage of research and development.

The diode test structures are manufactured with sensitive zones of two sizes: 2×2 mm^2 and 5×5 mm^2. The size of the sensitive zone of the smaller diode structure corresponds to that of a single strip.

2.4. TECHNOLOGICAL TEST STRUCTURES

Test structures are implemented on the wafer to monitor the technological process, for measuring the resistance of the layers of polysilicon, p^+- and n^+-implantations, for measuring contact resistance and other characteristics of the detector.

3. PROCESSING OF THE PROTOTYPES

3.1. SINGLE-SIDED DETECTOR PROCESSING

To manufacture the prototype of the p^+-side of a double-sided strip detector, one used four-inch wafers of n-silicon with resistivity of 3000-5000 Ohm·cm, <111> orientation and 350 μm thick, polished from both sides.

In the process of the first oxidation a pyrogeneous oxide 0.3 μm thick layer was grown at T=900°C with addition of HCl. This oxide was used as a mask during

ion implantation of phosphorus to form n^+-guard rings. Phosphorus ions with the energy E=60 keV and surface concentration 5×10^{14} at/cm^2 have been used. The back-side has also been implanted with phosphorus to make the Ohmic contact but with a higher surface concentration of ions 2.5×10^{15} at/cm^2.

After the formation of n^+-rings, the protective oxide was removed and a new protective oxide 0.6 µm thick was grown for masking during boron implantation. After formation of the pattern of p^+- regions, boron with the energy E=60 keV and surface concentration 5×10^{14} at/cm^2 was implanted. Phosphorus and boron ions were implanted through the layer of the dechanneling oxide 500 Å thick. After that, a SiO_2 layer 0.15 µm thick was grown as the first layer of a two-layer capacitor dielectric. The layer of a high temperature Si_3N_4 0.12 µm thick was the second one. To perform a comparative analysis, the Si_3N_4 layer was not deposited on some of the plates.

To form the resistors, a film of polycrystalline silicon 0.55 µm thick was deposited and doped by boron ion implantation up to the level required to obtain 1.5 MOhm resistors.

Contact holes to different layers (p^+, n^+ and polysilicon) were obtained by simultaneous wet etching the SiO_2 layers after lithographic formation of contact areas and plasma-chemical etching the Si_3N_4 layer in the region of contact areas.

Strip-detector metallisation was made by depositing Al with a small silicon admixture (1%). After lithographing aluminum, the passivating layer of the low temperature phosphorus-silicate glass 0.9 µm thick was deposited that covered the total surface of the detector. The photolithography over the passivating layer opened only Al areas of contact pads for connections to the detector and test structures. The final annealing of the detector was made at T=400°C in hydrogen during 30 min.

Up to now two sets of single-sided detectors were produced. In the first set, only double-layer insulation was used to create the coupling capacitors. In the second set, the silicon nitride was not deposited on some of the wafers. In all other respects, all the second set wafers are identical, processed according to the same technological operations.

3.2. DOUBLE-SIDED DETECTOR PROCESSING

The p^+-side processing of the double-sided microstrip detector is the same as the one used for the processing of the single-sided detector except for the absence of the Si_3N_4 additional insulation. Only single layer SiO_2 insulation with 0.25 µm thickness was used to create the coupling capacitors.

The n^+-strips have been implanted with phosphorus using a surface concentration of ions of 2.5×10^{15} at/cm^2. The common p^+-stop structure was formed by boron ion implantation at the energy of 60 keV and a dose of 5×10^{13} cm^{-2}. As the passivating layer, low temperature phosphorus-silicate glass 0.9 µm thick was deposited on the p^+- and n^+-sides of the detector.

4. TEST CONDITIONS

For measuring static characteristics the probe stations developed and constructed at KhIPT were used. A miniature mechanical adapter was also designed and produced to measure the characteristics of double-sided detectors before the readout electronics is mounted on them. The yield of good coupling capacitors was obtained using a semi-automatic probe station, because a lot of measurements are required by such tests.

4.1. MECHANICAL ADAPTER

A mechanical adapter was designed and produced to measure the static characteristics of double-sided microstrip detectors. The adapter is a mechanical device comprising two microposition probes (Fig. 3). The design provides for the arrangement of a silicon wafer, 4 inches in diameter, in the adapter. The wafer is embedded in a receptacle electrically insulated from the whole adapter structure. The plate is fixed by two fasteners with a uniform spring-load around the perimeter of the plate.

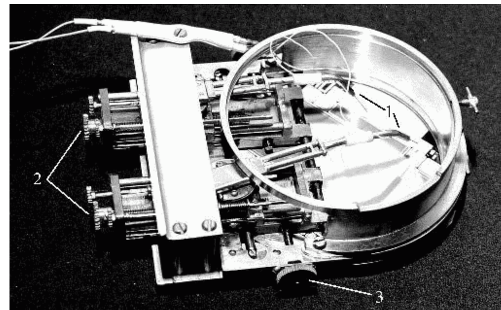

Fig. 3. *The mechanical adapter for static characteristics measurements of double-sided microstrip detectors. 1- two microposition probes, 2, 3- the control handles of the probes.*

The needles of both probes are insulated from the case and have the leads brought out to the instruments. The needles are moving independently of one another and can be put at any point within one-half the detector plate area. The needle is set in preliminary motion through a rough and rapid circular displacement (rotation) around the axis places at the center of the carriage. The final positioning of the needle is achieved by a precise movement of the carriage in two directions using screw pairs. The design of the microprobes permits the needles to be smoothly lowered and raised to a distance of 2 to 3 mm with respect to the plate surface.

The procedure of positioning the probes at the required site can be performed with any microscope having a focal distance of no less than 25 mm. After arranging the intrinsic probes in the required position and providing a contact, the adapter is flipped over, mounted on the platform of the measuring station and is fixed by clips (Fig. 4). The detector plate surface is fully

open on this side and the external probes of the measuring station can be placed at any point.

The microposition probes of the adapter are spring-loaded and are sufficiently rigid to provide a reliable contact between the needle and the plate. At the same time, the weight of the movable probe components is sufficiently small not to have the contact disrupted as the adapter is flipped over. The reliability of contacts was verified in the course of both, tests and measurements. A properly done contact has never failed.

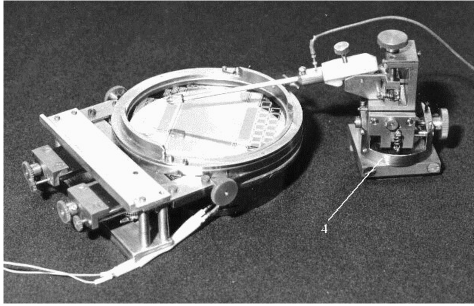

Fig. 4. *The adapter flipped over and the separated microposition probe (4).*

The flaw in the design of the adapter is that on lowering the probe needles into the plate the motion of the needle tip is not exactly perpendicular to the plate, and the needle position has to be corrected.

4.2. MEASUREMENT OF THE RADIATION TOLERANCE OF THE MICROSTRIP DETECTOR

As is known, the action of radiation on semiconductor detectors is implemented, mainly, via two mechanisms. The first mechanism of bulk damaging consists in breaking the crystal symmetry through displacing atoms from their lattice sites. The second mechanism of surface damage consists in changing the charge state of the Si/SiO_2 interface through the oxide ionization [2,3]. In view of this, to simulate the radiation conditions for the inner tracking system (ITS) of the ALICE detector, it is necessary to irradiate the detector with ~600 Gy of ionizing radiation and a neutron fluence of $\sim10^{11}$ n/cm^2 (corresponding to 10 years of ALICE operation). Namely, the neutrons simulate the action of high energy particles on the bulk of the detector material [4,5].

The radiation tolerance of microstrip detectors in this paper was studies using 20 MeV electrons in the Kharkov Institute of Physics and Technology.

The absorbed dose (Gy) in the specimen irradiated with electrons was determined using the well-known values of ionization energy losses and the measured integral densities of electron fluxes. The absorbed dose and its distribution over the detector were also measured with color film dose meters. The color film-ref dose meters permit one to perform measurements with an accuracy ≤20% under steady outer conditions and the temperature not exceeding 60ºC. The measurements of the optical density of dose meters were made with micro-photometers.

4.3. TEST OF 20 MeV ELECTRONS BULK DAMAGING EFFICIENCY

In the case of irradiation with high energy electrons, along with ionization, the action of electrons is determined by the generation of structure defects in the bulk of the crystal detector due to the displacement of substance atoms by accelerated electrons [2, 6, 7].

The efficiency of 20 MeV electron action on bulk material of the microstrip detector was determined from the change in the lifetime of charge carriers in silicon specimens-witnesses [6]. It is known that neglecting the influence of the surface one can determine the leakage current of a semiconductor detector from the relationship [8]

$$j=qn_jWA/2\tau, \quad (1)$$

where q is the electron charge, W is the depth of the detector depletion, A is the active region of the detector, τ is the effective minority carrier lifetime and n_j is the intrinsic carrier concentration. The expression for change of the leakage current of the detector normalized by one acting particle or one dose unit will have the form

$$\Delta j= 0.5qn_jWA\cdot\Delta\tau^{-1}/D, \quad (2)$$

similar to the well-known expression for the radiation constant of a semiconductor material [2]

$$K_\tau=\Delta\tau^{-1}/D, \quad (3)$$

Since the leakage current and the radiation constant of the detector material have similar dependencies on the carrier lifetime, then measuring the quantity K_τ for the detector material, one can judge on the efficiency of radiation action on a semiconductor detectors. Measuring K_τ was used in this paper for the determination of the relative efficiency of 20 MeV electrons required for the simulation of the action of 14 MeV neutrons with a given fluence on the bulk of the detector material. The measured data are given in Table 1.

Table 1. *Measurement of relative bulk damaging efficiency of 2 MeV and 3 MeV electrons, 14 MeV neutrons*

Particle	Energy, MeV	Measured K_τ, cm^2/s	K_τ [2], cm^2/s	Efficiency of electrons (relative to 14 MeV neutrons)
n	14	$1.5\cdot10^{-6}$	$1.5–2\cdot10^{-6}$	1
e	3	$1.5\cdot10^{-8}$	$\sim2\cdot10^{-8}$	0.01
e	20	$4.1\cdot10^{-8}$		0.027

The results obtained for K_τ for 3 MeV electrons and neutrons practically coincide with the results of the paper [2]. Using the efficiency value obtained we have assumed that the integral flux of 20 MeV electrons 40 times exceeding the fluence of 14 MeV neutrons exerts on the detector characteristics the close action. We believe our procedure of irradiation to be valid taking into account the rather low radiation environment in ALICE. The predicted changes in the detector characteristics as a result of irradiation are not large. Correspondingly, the value of the inverse annealing of detector characteristics as a result of restructuring the bulk clusters of defects after irradiation [2, 9, 10] is negligible.

5. RESULTS

The detector was irradiated in a non-biased state. The static characteristics of the detector were measured just before and after irradiation. Table 2 shows the initial characteristics of the produced single-sided and double-sided microstrip detectors. Fig. 5 shows the distribution of leakage currents and biasing resistor values for 750 strips detector with Si_3N_4 additional insulation.

5.1. DEPLETION VOLTAGE

Fig. 6 shows the bulk capacity against the depletion voltage for different irradiation doses. The depletionvoltage was studied with the capacitive technique [11] at 1 kHz and 1 MHz measuring frequency.

The voltage of total depletion was determined from the point where the strong and weak variations of capacity against voltage in log-log coordinates intersect.

Table 2. *Microstrip detectors characteristics*

Set	1996 set	1997 set		1998 set
Type	I	I	II	Double-sided
Design	Ion impl. single-sid. AC coupled structure with polysil. resistors and with oxide passivation	Identical	Identical	Ion impl. double-sided AC coupled structure with polysil. resistors and with oxide passivation
Technology	4 inch silicon	Identical	Identical	Identical
Si_3N_4 layer	+	+	-	-
Active area	40×75 mm^2	Identical	Identical	Identical
No of channel	750	750	750	750+750
Pitch	100 μm	100 μm	100 μm	100 μm
Interstrip Capacitance	4 pF	4 pF	4 pF	5 pF
Interstrip resistance	3 GOhm	3 Gohm	100 Gohm	43 GOhm (30 GOhm,10 rad)
Strip leakage current (FD)	20 nA	20 nA	1 nA	<2 nA (<5 nA, 10 krad)
Biasing resistor	1.8 MOhm	1.5 MOhm	1.5 MOhm	30 MOhm
Coupling capacitors	200 pF	200 pF	300 pF	120 pF
Capacitor breakdown	>100 V	>100 V	>25 V	>60 V
Number of dead strips (leakage current)	<1%	<1%	<1%	<1%
Number of broken capacitors	<1%	<1%	<3%	<2%
Number of work resistors	100%	100%	100%	100%

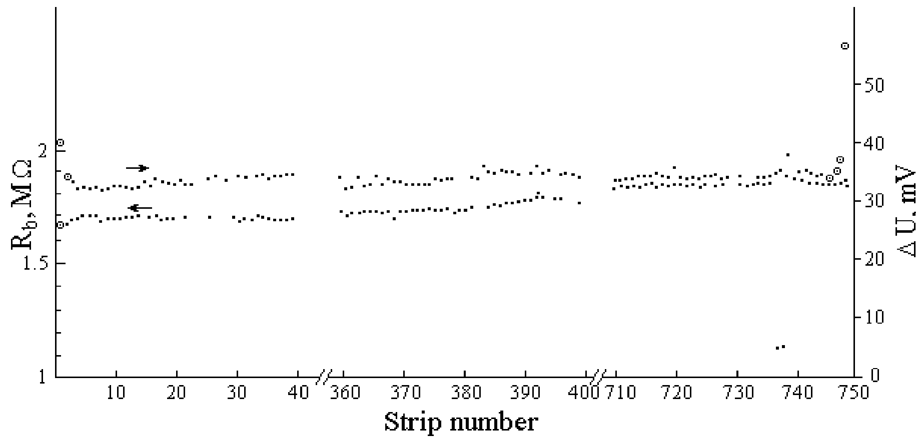

Fig. 5. Leakage current (voltage on the integrated resistors) and integrated resistor value distributions for 750 strips detector.

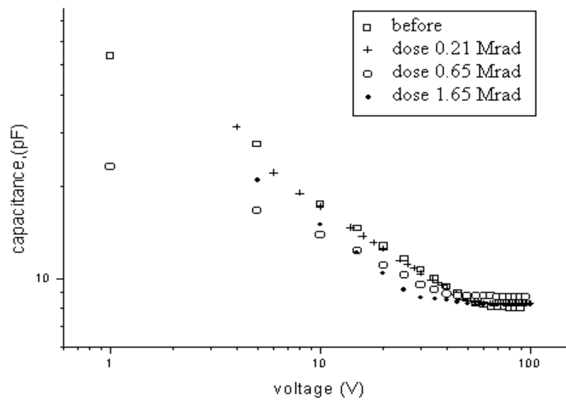

Fig. 6. Bulk capacity against the bias voltage for different integral doses.

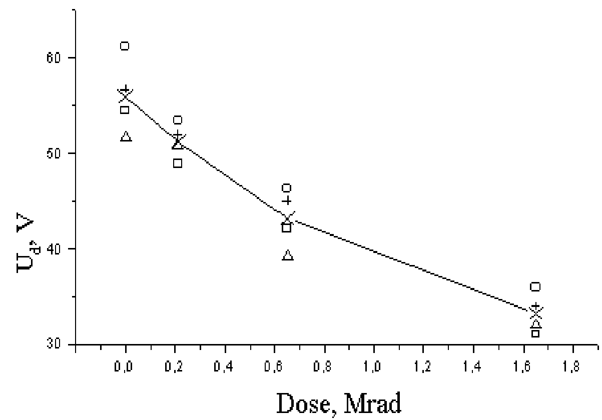

Fig. 7. Full depletion voltage for different irradiation dose. O, , Δ, +– are here the data for four different detectors.

Fig. 7 shows the full depletion voltage against the irradiation dose. The changes of the full depletion voltage are slight for the doses expected in the ALICE experiment. One observes no change of the conductivity type in the range of doses under study.

5.2. LEAKAGE CURRENTS

5.2.1. INCREASE OF LEAKAGE CURRENTS OF THE DOUBLE-SIDED MICROSTRIP DETECTOR AFTER 10 krad DOSE

The radiation tolerance of the double-sided microstrip detector was studied for a 10 krad dose using 20 MeV electrons. The leakage current increases from 2 up to 5 nA per strip (Fig. 8).

Together with the detector a silicon specimen-witness, having characteristics similar to those of the detector, was irradiated. Using the specimen-witness one has the possibility to control the conditions of irradiation by comparing the measured radiation damage constant K_τ with the results obtained previously. It is well-known, that the $1/\tau=f(D)$ dependence in a wide dose range has a linear character that is very convenient for determining the damage constant K_τ. The irradiation of the specimen-witness was performed also with the aim to estimate the influence of surface and other effects on the change of leakage current during irradiation. The 8 mm thickness of the silicon specimen was selected sufficiently high so that the lifetime of minor charge carriers τ_{NCC} can be measured without taking into account the surface influence of the commonly used contactless RF-method. At the same time, the silicon thickness was sufficiently small for neglecting the electron energy losses over the specimen thickness under irradiation.

The lifetime of minor charge carriers in the detector material bulk was obtained from the relationship (1) in the prediction that the total leakage current is determined by the generation in the bulk material.

It is seen from the Fig. 8 that the initial lifetime of minor charge carriers in the detector material, determined by the leakage current, is less than the initial one in the silicon specimen-witness. As is well-known the decrease of the τ value in a detector is due to the leakage current which appears because of surface

imperfection and because of additional recombination centers in Si in the process of detector construction

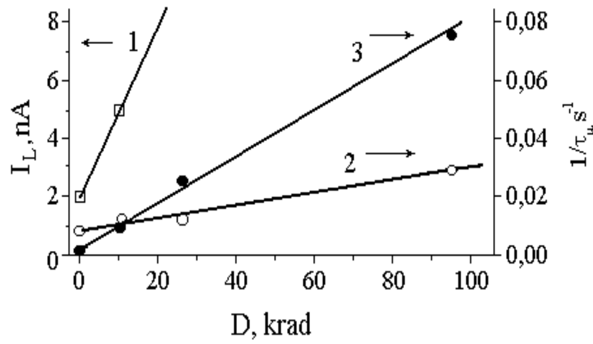

Fig. 8*. Leakage current (1), inverse lifetimes (2) in DSMD and inverse lifetime (3) in the silicon specimen as a function of the dose***.

In Fig. 8 are plotted the inverse lifetimes $1/\tau$ in the silicon specimen and the detector as a function of the irradiation dose. The damage constant for the silicon specimen determined from the dependence of the inverse lifetime on dose is in good agreement with the previous results (Table 1 and [2]).

The comparison of the values of the slope of $1/\tau = f(D)$dependences show that the radiation resistance of the detector is higher than that of the initial silicon. Probably, it can be explained by the heterogeneity of the detector surface as well as by the annihilation centers in the material bulk created in the process of technological treatment.

5.2.2. LEAKAGE CURRENTS OF SINGLE-SIDED DETECTORS AT HIGH IRRADIATON LEVEL

The leakage currents for single-sided microstrip detectors (p^+-side of the double-sided detector) were studied in wider dose intervals. Single-sided detectors with and without additional layer of Si_3N_4 insulator were made in one set, using the same thickness for the SiO_2 insulator. The additional Si_3N_4 layer allows a coupling capacitor breakdown voltage larger than 100 V and capacitor yield larger than 99 percent. However, the leakage current for detectors with double layer insulator is about 20 nA per strip while the leakage current for the single layer SiO_2 insulated detectors is only 2 nA (Table 2). The 20 nA leakage current leads to additional noise, 450 electrons when the ALICE 128C electronics with a peaking time of 1.4 microseconds is used. At a 1 nA leakage current the noise is 100 electrons. The ENC for an input capacitance of 5 pF is 300 electrons.

Perhaps, the increase of the leakage current for the detectors with the silicon nitride is associated with the increase of the surface generation-recombination centers on the open surface, and, especially, over the strip perimeter at the contact of the open surface and p^+-strip. The leakage current dependence on diode dimensions may support this viewpoint. Increasing the sensitive zone of the diode, the leakage current normalized by the unit of sensitive area decreases for diodes with Si_3N_4.

Increasing the sensitive zone area, the ratio of the open surface of the detector (surface between the p^+-guard ring and p-implanted zone of the diode) to the sensitive area of the diode decreases. The ratio of the perimeter to the area of the sensitive zone also decreases. For the diodes without additional Si_3N_4 insulation layer the leakage currents normalized by the unit area are practically constant. Moreover, the value of the normalized current for the diode coincides with the one for the microstrip detector.

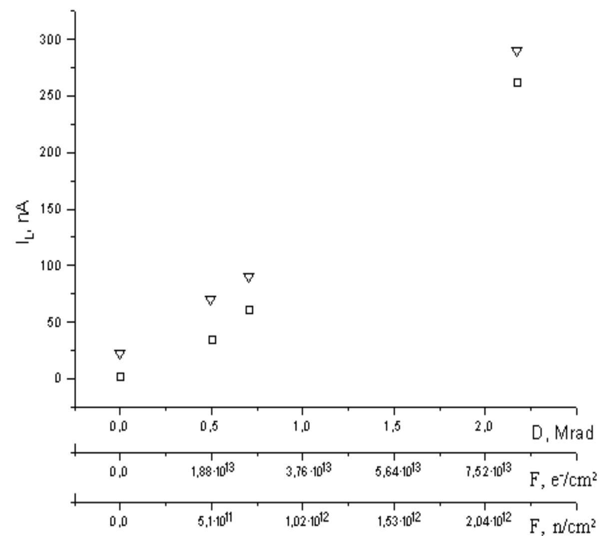

Fig. 9*. Leakage currents variation for microstrip detectors with (∇) and without Si_3N_4 ( ).*

Fig. 9 shows the variation of leakage currents for microstrip detectors with and without Si_3N_4 under irradiation with 20 MeV electrons. One sees that these dependences are almost linear. Furthermore, the initial difference in current of ~20 nA observed for the detector with Si_3N_4 persists over the entire range of doses. It has to be pointed out that the large initial difference gets relatively much smaller at large irradiation doses. Fig. 10 shows the distribution of leakage currents for microstrip detectors with Si_3N_4 and without it before irradiation and after irradiation with the maximum dose. One sees that a good uniformity of the distribution of leakage currents persists after the maximum irradiation dose.

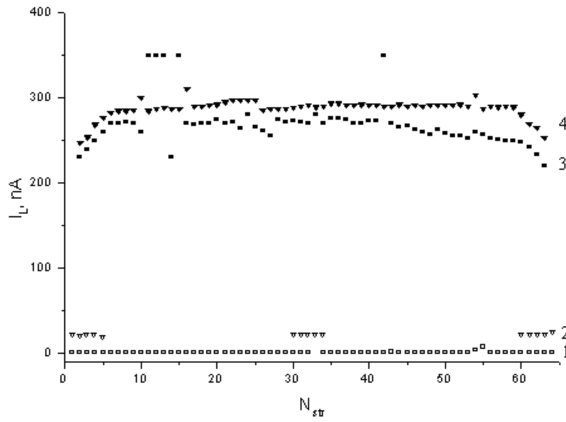

Fig. 10. *Leakage currents distributions before (1, 2) and after (3, 4) irradiation. 1, 3 - single-layer and 2, 4 - double-layer insulation.*

It was shown that for single-sided silicon microstrip detectors on 4000 Ohm·cm n-type silicon the use of the Si_3N_4 insulation layer increased the leakage current from 1 nA/strip to 20 nA/strip. However, this increase in leakage current is small compared to the increase of leakage current induced by a less that 1 Mrad irradiation doses. After a 2 Mrad dose the leakage currents of both types of detectors were approximately 250 nA/strip

5.3. INTERSTRIP RESISTANCE

Fig. 11 shows the interstrip resistance for detectors with single-layer and double- layer insulation against irradiation dose. The same figure shows the variation of the ratio of interstrip resistances for the detectors with single-layer and double-layer insulation.

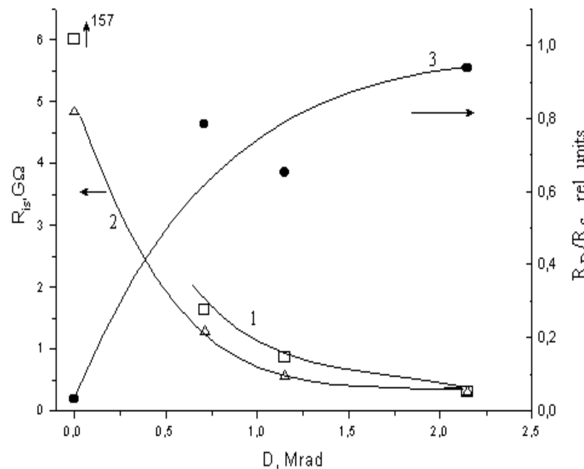

Fig. 11. *Interstrip resistance for the detectors without (1) and with (2) Si_3N_4. Interstrip resistances ratio for the detectors with double-layer and single-layer insulation (3).*

Naturally, the surface conductivity, created by surface generation-recombination centers in the detectors with additional insulation, decreases the initial value of the interstrip resistance. However, one sees that the surface effect on the interstrip resistance also becomes insignificant already at irradiation doses < 1 Mrad.

5.4. INTERSTRIP AND TOTAL STRIP CAPACITANCE

The large strip pitch (the strip pitch 100 μm and interstrip gap 60 μm) of the detector provides for small value of the interstrip and total strip capacitances. Perhaps, owing to the same reason, the interstrip capacity and total capacity of the strip show weak dependence on the irradiation dose.

6. CONCLUSIONS

The technology of production of DSMD at the KhIPT has been mastered. Test of the static characteristics on the first batch of ALICE prototype detectors has been made, as well as a study of the radiation damage under a 10-years ALICE equivalent dose.

The main results show that:

1. The number of defective strips does not exceed 3%.

2. The leakage current increases from 2 up to 5 nA per strip and the interstrip resistance decreases from 43 down to 30 GOhm after a 10 krad irradiation dose. The other DSMD features remain unchanged under irradiation.

Having in mind that the first batch was small and experimental, we have been starting a second batch to get more representative estimates both on the production yield and on the detector efficiency.

ACKNOWLEGEMENTS

The authors are very thankful to many colleagues for the valuable discussions and constructive remarks, especially P. Giubellino and O. Runolfsson. This work was supported by INTAS under the Grant 96-0678.

REFERENCES

1. A.P. de Haas, P. Kuijer, V. Kulibaba, N. Maslov, V. Perevertailo, S. Potin, A. Starodubtsev. Radiation tolerance of single-sided microstrip detector with Si_3N_4 insulator. *ALICE/PUB 98-24*, 5 Nov. 1998.
2. H.W. Kraner, *Nucl. Instr. and Meth. A225*, 1984, p. 616-618.
3. J. Kemmer and G. Lutz. *Nucl. Instr. and Meth. A273*, 1988, p. 588.
4. *Technical Proposal for A Large Ion Collider Experiment at CERN LHC. CERN/LHCC/95-71*, 15 December 1995.
5. A. Holmes-Siedle, M. Robbins, S Watts et al. *Nucl. Instr. and Meth. A339*, 1994, p. 511-523.
6. N. Maslov, G. Bochek, V. Kulibaba et al. *ALICE/95-19, Internal Note/SIL*, 15 June 1995.
7. N.I Maslov, G.D. Pugachev, M.I. Heifets. *Physics and Technics of Semiconductors.* 1982, v. 16, No 3, p. 513-515.
8. A.S. Grove, *Physics and Technics of Semiconductor Devices, New York, Wiley*, 1967, Ch. 6, p. 176-177.

9. I.D. Konozenko, A.K. Semenyuk and V.I. Khivrich. *Radiation effects in semiconductors, eds.,* J.W. Corbett and G.D. Watkins, (Gordon and Breach, London, 1971).
10. E. Fretwurst, H. Feick, M. Glaser et al., *Nucl. Instr. And Meth.* 1994, v. *A342,* p. 119-125.
11. M.A. Frautschi et al., Capacitance *Measurements of Double-Sided Silicon Microstrip Detectors, The New Mexico Center for Particle Physics CDF Collaboration note CDF/DOC/SEC_VTX/ CDFR/2546.*